OXFORD GENETICS

GENETICS, 2024, 227(4), iyae084
https://doi.org/10.1093/genetics/iyae084
Advance Access Publication Date: 19 May 2024
Investigation

Analysis of meiotic recombination in *Drosophila simulans* shows no evidence of an interchromosomal effect

Bowen Man,[1] Elizabeth Kim,[2] Alekhya Vadlakonda,[1] David L. Stern,[2] K. Nicole Crown [1,*]

[1]Department of Biology, Case Western Reserve University, Cleveland, OH 44106, USA
[2]Janelia Research Campus, Howard Hughes Medical Institute, Ashburn, VA 20147, USA

*Corresponding author: Department of Biology, Case Western Reserve University, 112 Millis Hall, 2074 Adelbert, Cleveland, OH 44106, USA. Email: knc38@case.edu

Chromosome inversions are of unique importance in the evolution of genomes and species because when heterozygous with a standard arrangement chromosome, they suppress meiotic crossovers within the inversion. In Drosophila species, heterozygous inversions also cause the interchromosomal effect, whereby the presence of a heterozygous inversion induces a dramatic increase in crossover frequencies in the remainder of the genome within a single meiosis. To date, the interchromosomal effect has been studied exclusively in species that also have high frequencies of inversions in wild populations. We took advantage of a recently developed approach for generating inversions in *Drosophila simulans*, a species that does not have inversions in wild populations, to ask if there is an interchromosomal effect. We used the existing chromosome 3R balancer and generated a new chromosome 2L balancer to assay for the interchromosomal effect genetically and cytologically. We found no evidence of an interchromosomal effect in *D. simulans*. To gain insights into the underlying mechanistic reasons, we qualitatively analyzed the relationship between meiotic double-stranded break (DSB) formation and synaptonemal complex (SC) assembly. We found that the SC is assembled prior to DSB formation as in *D. melanogaster*; however, we show that the SC is assembled prior to localization of the oocyte determination factor Orb, whereas in *D. melanogaster*, SC formation does not begin until the Orb is localized. Together, our data show no evidence that heterozygous inversions in *D. simulans* induce an interchromosomal effect and that there are differences in the developmental programming of the early stages of meiosis.

Keywords: *Drosophila simulans*; inversion; meiosis

Introduction

Chromosome inversions are of unique importance in the evolution of genomes and species because when heterozygous with a standard arrangement chromosome in an individual, they effectively suppress meiotic crossover formation within the inversion (Sturtevant 1926; Stone and Thomas 1935; Sturtevant and Beadle 1936). Crossovers do form within an inversion but result in chromosome rearrangements that cause aneuploid (and thus inviable) gametes, preventing inheritance of the recombinant chromosome in the next generation (Sturtevant 1926; Stone and Thomas 1935; Sturtevant and Beadle 1936). Crossover suppression has consequences for fertility on the single generation time scale because crossovers are essential for meiotic chromosome segregation and over long evolutionary timescales because suppressing crossovers affects the rate of gene flow within and across populations (Noor *et al.* 2001; Rieseberg 2001).

In *Drosophila* species, heterozygous inversions have an additional effect during meiosis termed the interchromosomal effect, whereby the presence of a heterozygous inversion induces a dramatic increase in crossover frequencies in the remainder of the genome in a single generation (comprehensively reviewed in Lucchesi and Suzuki 1968). In *Drosophila melanogaster*, the interchromosomal effect is caused by activating the pachytene checkpoint and extending the developmental window where prophase (and crossover formation) occurs, ultimately leading to a 50–500% increase in crossover frequencies on the noninverted chromosomes (Joyce and McKim 2010). The increase in crossover frequencies is not caused by increasing the number of meiotic DNA double-stranded breaks (DSBs); rather there is a shift in the balance between crossover and noncrossover repair outcome during meiotic recombination (Joyce and McKim 2010; Crown *et al.* 2018).

The molecular consequences of heterozygous inversions and the interchromosomal effect have far ranging impacts on the rate of gene flow within and between populations. Gene flow is reduced locally between the inversion and the standard arrangement chromosome but is increased in the remainder of the genome. Since many Drosophila species are polymorphic for inversions in wild populations, understanding the molecular mechanisms and the pervasiveness of the interchromosomal effect is important for understanding how inversions shape populations. Various estimates have shown that inversions occur at very high frequencies in multiple Drosophila species. Perhaps the most informative estimate is the number of species within a subgenus that are monomorphic or polymorphic for inversions

Received on 09 March 2024; accepted on 09 May 2024

(Powell 1997; Aulard et al. 2004). Within the Drosophila subgenus, approximately half of the species are polymorphic for inversions (41 species) and half are monomorphic (44 species). Within the Sophophora subgenus, 38 species are polymorphic for inversions (including *D. melanogaster*), while only five are monomorphic (*D. simulans*, *D. mauritiana*, *D. sechellia*, *D. erecta*, and *D. santomea*). It is striking that within the *D. melanogaster* species subgroup, the simulans species complex is monomorphic (*D. simulans*, *D. mauritiana*, and *D. sechellia*), while their sister species *D. melanogaster* is highly polymorphic (Powell 1997; Aulard et al. 2004).

It is surprising that such closely related species within the *D. melanogaster* species subgroup have dramatically different frequencies of inversions. Previous work has attempted to explain this difference at the molecular level by asking if *D. simulans* and *D. melanogaster* differ in their response to repairing DSBs and found conflicting results. Woodruff and Ashburner irradiated male flies with 4,000 rads of ionizing radiation and found the same number of chromosome aberrations (translocations and inversions) in both species (Woodruff and Ashburner 1978). However, Lemke performed the same experiment and found chromosome aberrations in 24.8% of the offspring from *D. melanogaster* and only 0.8% from *D. simulans* (Lemke et al. 1978). A later experiment by Inoue also found about half as many chromosome breaks in *D. simulans* compared with *D. melanogaster* after exposure to ionizing radiation (Inoue 1988). Additionally, *D. simulans* has been resistant to karyotype manipulation in the lab. Despite exhaustive attempts to generate balancer chromosomes using the same methods that have been successful in *D. melanogaster*, all attempts that we are aware of have failed (Stern 2022).

Recently, a doubly inverted chromosome 3R balancer (*j3RM1*) was successfully generated in *D. simulans* using an elaborate site-specific recombination approach that screened for loss and gain of fluorescent markers, which allowed 5,000–10,000 flies to be screened in each step of the process (Stern 2022). In the work presented here, we generated an additional chromosome 2L doubly inverted balancer (*j2LM1*) and used it and *j3RM1* to ask if the interchromosomal effect is present in a species that is normally monomorphic for inversions in the wild. Using recessive marker scoring to determine crossover frequencies, we found no evidence of an interchromosomal effect. We also found no evidence of pachytene checkpoint activation in response to heterozygous inversions in this species, additionally suggesting there is no interchromosomal effect. We did find differences in the developmental timing of early meiosis in *D. simulans* compared with *D. melanogaster* and suggest that this difference is one of several possible explanations for why there is no interchromosomal effect in this species.

Methods

Drosophila stocks and husbandry

All *D. simulans* stocks were maintained at 25°C on standard cornmeal media. w^{501} (stock #14021-0251.11), $y^1\ v^2\ f^1\ bb^1$ (stock #14021-0251.147), and $ju^1\ st^1\ e^1\ p^1$ (stock #14021-0251.174) stocks were obtained from the National Drosophila Species Stock Center. We note that chromosome 3R in *D. melanogaster* is inverted relative to *D. simulans* (Courret et al. 2019), so the gene order for *e* and *p* is reversed relative to *D. melanogaster*. In our hands, bb^1 was no longer visible in the $y^1\ v^2\ f^1\ bb^1$ stock. Kenya C157.4 was a gift from Amanda Larracuente. The third chromosome inversion *j3RM1* was previously published and is maintained as *dsx/j3RM1* (Stern 2022). All stocks are listed in the Supplementary Reagents Table (Supplementary File 2).

Generating the *j2LM1* balancer stock

We followed the protocol described in Stern (2022) to generate 2 overlapping inversions on chromosome arm 2L in *D. simulans*. Four plasmids carrying reporter genes expressing variously colored fluorescent proteins in different anatomical regions and either FRT or KD yeast recombination sites were integrated separately into existing attP landing sites in *D. simulans* (Stern et al. 2017): sim-2810 p{ie1-dsRed::FRT-RC,attB} into sim-952 p{attP, 3XP3-EYFP} inserted at 2L: 830,996; sim-2720 p{MHC-EGFP::KD} into sim-1048 p{attP, 3XP3-EYFP} inserted at 2L: 6,392,252; sim-2664 p{3XP3-DsRed::FRT} into sim-1230 p{attP, 3XP3-EYFP} inserted at 2L: 13,194,453; and sim-2719 p{MHC-DsRed::KD-RC} into sim-960 p{attP, 3XP3-EYFP} inserted at 2L: 22,086,768. All genome coordinates are relative to *D. simulans* genome assembly NCBI:GCA_016746395.1. All four transgenes were recombined onto a single chromosome arm. Flies carrying all four transgenes on a single chromosome were crossed to flies carrying a source of heat-shock inducible Flipase p(MUH-HES-FLPL, w+, attB) integrated into 1029-simD-234.5 at 3R: 17,461,328. Plastic vials containing developing larvae in their food media were placed in a 37°C bead bath (Lab Armor) for 1 h, followed by 1 h at room temperature, and a second 37°C heat shock for one hour. Male progeny were crossed to a *w-* strain of *D. simulans* and offspring of this cross were screened for loss of ie1-DsRed and 3XP3-dsRed, but retention of MHC-EGFP and MHC-DsRed, which indicates inversion between the FRT sites. Flies carrying this singly inverted chromosome were then crossed to flies carrying a source of heat-shock inducible KD recombinase p(MUH-HES-KD::PEST, w+, attB) integrated into 2176-simD-299.6 at 2L:6,583,842. This attP landing site is derived from 1048-simD-299.6, but has had its 3XP3-EYFP marker inactivated by CRISPR–Cas9 mutagenesis of the EYFP gene (Stern et al. 2017). Larvae from this cross were heat shocked as described above, and adults were crossed to a *w*-strain of *D. simulans*. Offspring were screened for loss of MHC-EGFP and MHC-DsRed, but presence of 3XP3-EYFP, which is present in all four landing sites with integrated recombination plasmids, but not in the landing site with the KD-recombinase integrated. These progeny carried presumptive double-inversions on Chromosome 2L, which we named *j2LM1*.

To determine whether *j2LM1* might serve as a useful balancer chromosome, flies carrying this chromosome were backcrossed to a *w*-strain of *D. mauritiana* for 10 generations. The presence of the balancer was confirmed in flies of every generation by expression of EYFP in the eyes. Twelve independent backcrosses were performed, and DNA was prepared from one individual of the tenth generation from each backcross and subjected to multiplexed-shotgun genotyping to estimate chromosome ancestry (Andolfatto et al. 2011). Sequencing libraries were prepared from DNA using tagmentation (Picelli et al. 2014), sequenced on an Illumina platform, and sequencing reads were provided as input to the multiplexed shotgun genotyping software described in Andolfatto et al. (2011). All progeny were heterozygous for chromosome 2L, indicating that *j2LM1* prevented inheritance of recombination events on chromosome 2L (Fig. 1).

Immunofluoresence

About 2–3-day-old mated females were put on yeast paste overnight. Ovaries were dissected in PBS and fixed for 20 min in 1,000 µl of solution containing 2% paraformaldehyde (Ted Pella cat. no. 18505), 0.5% Nonidet P-40 (Sigma cat. no. I8896), 200 µl

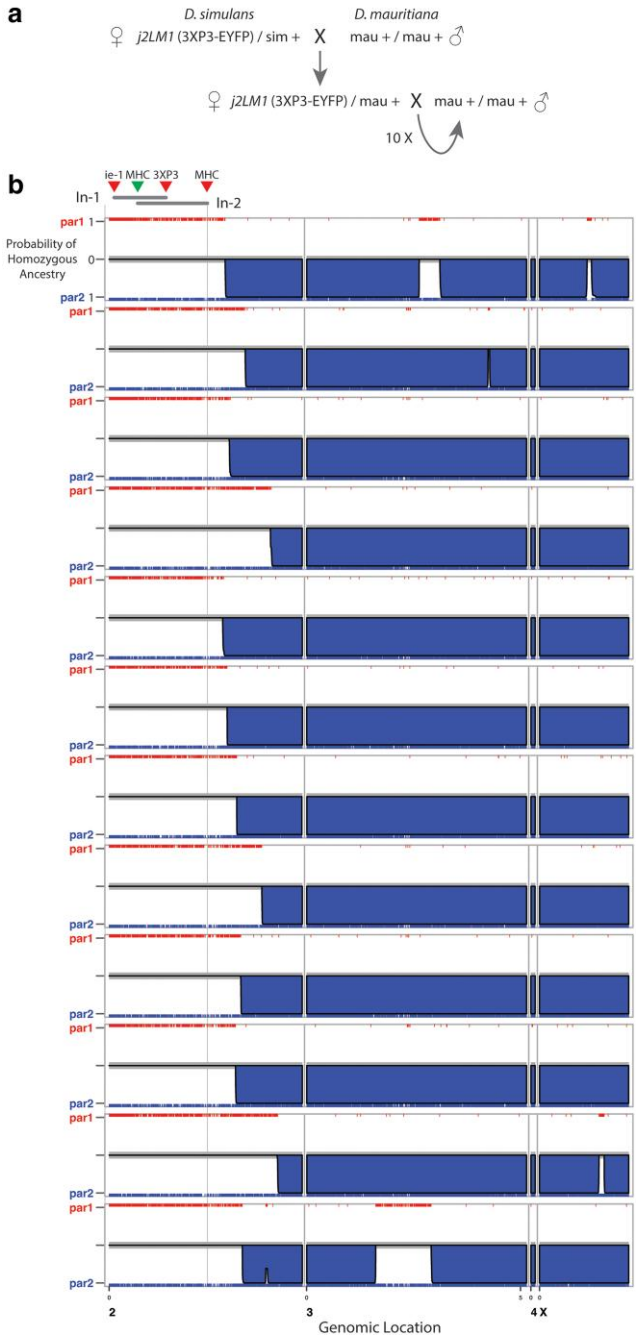

Fig. 1. Results of testing for the ability of *j2LM1* to prevent inheritance of recombination events and serve as a balancer chromosome. a) Flies carrying *j2LM1* (3XP3-EYFP) were crossed to *D. mauritiana* males and then hybrid flies were backcrossed to *D. mauritiana* males for 10 generations. A total of 12 independent crosses were performed. b) Single flies carrying *j2LM1* (3XP3-EYFP) were sampled from each backcross after 10 generations of backcrossing and subjected to Multiplex Shotgun Genotyping (Andolfatto *et al.* 2011). Ancestry plots for each of the 10 individuals are shown. Par1 is probability of homozygous *D. simulans* ancestry, which would be shown in red if any regions displayed homozygous homozygous *D. simulans* ancestry. Par2 is probability of homozygous *D. mauritiana* ancestry, shown in blue, revealing that many genomic regions have become homozygous for *D. mauritiana* DNA after 10 generations. In all flies, the left side of Chromosome 2 shows heterozygous ancestry (0 probability of homozygous ancestry for either parent), indicating that *j2LM1* prevents inheritance of recombination events in this chromosomal region. In all lines, the region of heterozygosity extends for several Mb proximal to the most proximal breakpoint of the *j2LM1* balancer, suggesting that recombination is suppressed also proximal to this breakpoint.

PBS, and 600 µl heptane. Ovaries were then washed 3 times for 10 min each in PBS with 0.1% Tween-20 (PBST), blocked for 1 h at room temperature in PBS with 1% BSA (MP Biomedicals cat. no. 152401), and incubated with primary antibody diluted in PBST overnight at 4°C. The ovaries were then washed 3 times in PBST and incubated in secondary antibody diluted in PBST for 4 h at room temperature. DAPI was added for the last 10 min at a concentration of 1 µl/ml. The ovaries were washed again 3 times for 15 min each in PBST. All wash steps and antibody incubations were done while nutating. The ovaries were mounted in ProLong Glass (Invitrogen cat. no. P36980) and allowed to cure for the manufacturer's suggested time.

Since *D. simulans* is closely related to *D. melanogaster*, we reasoned that some antibodies against *D. melanogaster* proteins would work in *D. simulans*. We found that the following *D. melanogaster* antibodies result in similar staining patterns in *D. simulans* as in *D. melanogaster*: anti-Corolla (Collins *et al.* 2014), anti-phospho-H2AV (Lake *et al.* 2013), and anti-Orb (Lantz *et al.* 1994). We used rabbit anti-Corolla at 1:3,000 (gift from Scott Hawley), mouse anti-phospho-H2AV at 1:500 (DSHB clone UNC93-5.2.1), and mouse anti-Orb at 1:20 (DSHB clone 6H4 at 1:40 combined with clone 4H8 at 1:40). We used the following secondary antibodies: Goat anti-Mouse IgG2b Alexa Fluor 594 (Thermofisher # A-21145), Goat anti-Mouse IgG1 Alexa Fluor 488 (Thermofisher #A-21121), and Goat anti-Rabbit Alexa Fluor 647 (Thermofisher #A-21244). All reagents are listed in the Supplementary Reagents Table (Supplementary File 2).

The ovaries were imaged on a Leica Stellaris 5 confocal microscope using an HC PL APO 63×/1.4 NA Oil objective. Images were acquired using the Lighting module with an Airy pinhole size of 0.75 Airy Units and the standard default settings dictated by the pinhole size. All images were deconvolved using the Leica Lightning internal software with default settings.

Measuring the frequency of two oocytes

To determine how many oocytes were present in region 3, we used maximum projections of the z-stack. For Orb staining, we categorized a germarium as having 1 oocyte if Orb was concentrated in the cytoplasm of a single cell in region 3. We categorized it as having 2 oocytes if Orb was concentrated in the cytoplasm of 2 cells; in these cases, Orb was often found in the cytoplasm of 2 cells but centralized between the 2 nuclei. For Corolla staining, we categorized a germarium based on the presence of full-length Corolla in 1 or 2 nuclei in region 3; if there was fragmented Corolla staining in 1 nucleus, we did not categorize this as having 2 oocytes, consistent with previous work analyzing the two-oocyte phenotype (Joyce and McKim 2010). Percentages were calculated as the number of germarium with 2 oocytes divided by the total number of germaria analyzed.

Crossover scoring

We used recessive marker scoring to analyze crossover frequencies. We crossed *jv st e p*/+ females to *jv st e p* homozygous males and scored offspring for each of the recessive markers. Crossovers were identified as locations where the genotype switched from mutant to wildtype. These crosses were performed in a wildtype background or in females that were heterozygous for a balancer. Some stocks contained a *white* mutation, and in these cases, only female offspring were scored. The same crosses were repeated to measure crossover frequencies on the X chromosome using a *y v f bb* chromosome.

The *j2LM1* stock is maintained over a wildtype chromosome 2, which allowed us to control for genetic background by measuring

crossover frequencies in wildtype and inversion siblings from the same cross. We crossed *w–*; *+/j2LM1* females to *y v f b* or *jv st e p* males. We recovered females that were heterozygous for the marker chromosome and either heterozygous for *j2LM1* (marked by 3xP3-GFP) or homozygous for the standard arrangement chromosome (marked by the absence of 3xP3-GFP). We crossed these females to *y v f b* or *jv st e p* males and scored crossovers in the offspring.

Statistics

Crossover frequencies were compared between two genotypes using Fisher's exact test and Bonferonni's correction for multiple tests. When three genotypes were compared simultaneously, a χ^2 test was performed. All statistical tests were performed in GraphPad Prism version 10.2 for Mac (GraphPad Software, Boston, MA USA).

To determine the effect size (change in crossover frequencies) we could detect given our sample sizes, we performed a sensitivity analysis using G*Power (v3.1, Faul *et al.* 2007). We carried out the sensitivity analysis using the following settings: test type was set to "exact – proportions: inequality, two independent groups Fisher's exact test", tail(s) was set to 2, effect direction was set to $p1 < p2$, power $(1 - \beta)$ was set to 0.9, and alpha error probability was set to 0.05. For each interval, the crossover frequency as a proportion in the inversion heterozygote was entered as $p2$ and the total sample sizes were entered. G*Power reports the minimum proportion $p1$ (crossover frequency in wildtype) that can be detected. The percent change between actual $p2$ and the minimum detectable $p1$ is reported in Supplementary Table 3 (in File 1) and represents the minimum percent difference between map lengths that we had power to detect in our data set.

Protein sequence alignment

The *pch2* ortholog in *D. simulans* was identified by performing a BLAST search against the *D. simulans* genome with the *D. melanogaster pch2* nucleotide sequence (Altschul *et al.* 1990). This identified the *D. simulans* gene LOC6728923 as *pch2*. We aligned the *D. simulans* and *D. melanogaster* predicted protein sequences in Geneious (version 2022.1.1, http://www.geneious.com/) using the pairwise alignment Geneious default settings, and annotated predicted functional domains manually based on Ye *et al.* (2015).

Results

Generating inversions in *D. simulans*

To ask if there is an interchromosomal effect in *D. simulans,* we took advantage of a multiply inverted third chromosome balancer that was recently generated (Stern 2022). This balancer, termed *j3RM1*, has 2 nested inversions that cover the entirety of chromosome 3R (Fig. 2). Importantly, the left arm of this chromosome is not inverted and thus it only balances the right arm. We also generated a new chromosome 2L balancer chromosome (*j2LM1*) that has 2 nested inversions on the left arm of chromosome 2 (see Methods for details). Similarly to *j3RM1*, the right arm of *j2LM1* is not inverted (Fig. 2).

To ensure that *j2LM1* does indeed suppress the inheritance of crossing-over events, we crossed females heterozygous for *j2LM1* to its sister species *D. mauritiana*, and then backcrossed the F1 offspring to *D. mauritiana* for 10 generations in 12 independent lines. Thus, recombination between *D. simulans and D. mauritiana* chromosomes was possible in every generation. We selected on the 3XP3-EYFP marker in every generation in females to ensure the inheritance of the balancer. We sequenced 1 fly from each of the 12 lines and determined if they were heterozygous or homozygous for *D. simulans* and *D. mauritiana* single nucleotide polymorphisms (SNPs). Regions where heterozygosity was maintained for 10 generations indicated crossovers did not form or were not inherited. We found each of the 12 lines was heterozygous for *D. simulans* and *D. mauritiana* SNPs in the portion of chromosome 2L with the inversion (Fig. 1). Most of the remainder of the genome in each individual was homozygous for *D. mauritiana* SNPs.

Although we previously showed that *j3RM1* suppresses crossovers using the same *D. mauritiana* backcross scheme just described, we used recessive marker scoring to confirm that this balancer suppresses crossovers within species. We crossed *j3RM1* to the multiply marked scoring chromosome containing *jv st e p* and found no crossovers in the *e – p* interval, which is included within the *j3RM1* inverted regions (Table 1; Supplementary Table 1 in File 1). Crossover frequencies were statistically the

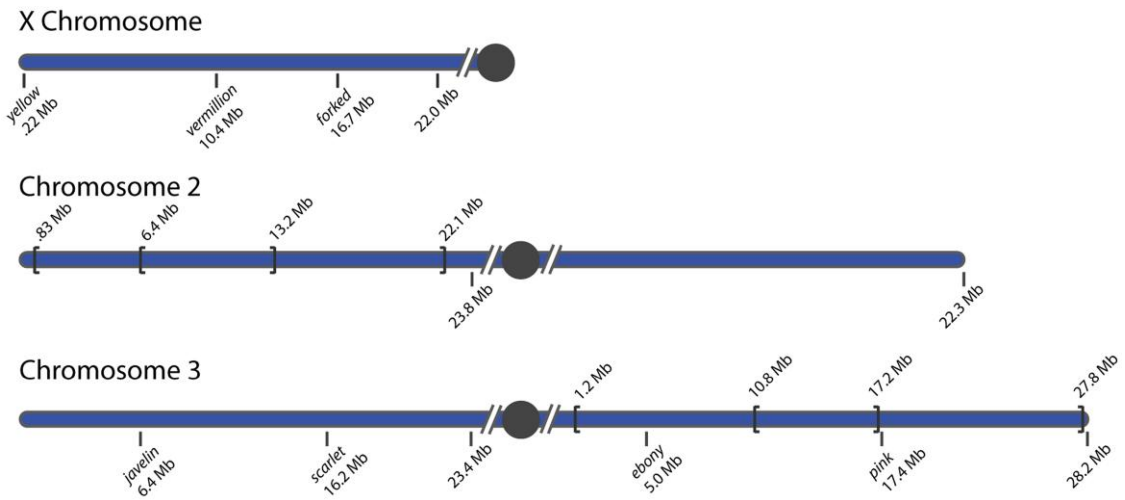

Fig. 2. Chromosome sizes, positions of the recessive markers, and location of inversion breakpoints used in this study. Recessive markers and their physical position are shown below the chromosomes. Inversion breakpoints are depicted as brackets and their physical position is listed above the chromosome. The end of each chromosome assembly is shown below the chromosome. All physical positions were obtained from the *D. simulans* genome NCBI:GCF_016746395.2 Black circles represent the location of centromere. Hashed lines represent unassembled pericentric heterochromatin of unknown size.

same as wildtype in the *jv–st* and *st–e* intervals, showing that there is no intrachromosomal effect from inversions as has been occasionally reported for *D. melanogaster* (Sturtevant and Beadle 1936; Grell 1964; Miller 2020).

Significant variation in crossover rates between wildtype stocks

D. melanogaster shows considerable intraspecies variation in crossover rates (Hunter *et al.* 2016). To determine crossover rates in various wildtype *D. simulans* strains, we used recessive marker scoring on chromosome 3 in 3 different wildtype strains: Kenya C167.4, w^{501}, and a full sibling wildtype strain derived from the *j2LM1* stock. We found statistically significant variations in crossover frequencies across all 3 genotypes (Table 1; Supplementary Table 1 in File 1, Chi-square test, $P < 0.0001$), with an overall map length of 68.93 cM in Kenya C167.4, 88.40 cM in w^{501}, and 79.52 cM in the full sibling wildtype strain. The variation in crossover frequencies occurs in all 3 individual intervals and no one interval can account for all variations. This variation in crossover frequencies between wildtype strains, combined with the recent discovery of high levels of pericentromeric genome instability in w^{501} (Courret and Larracuente 2023), led us to compare crossover frequencies in wildtype full siblings whenever possible.

There is no evidence of an interchromosomal effect in *D. simulans*

To determine if there is an interchromosomal effect in *D. simulans*, we looked for differences in crossover frequency on chromosome 3 in females heterozygous for the *j2LM1* inversion and in wildtype full siblings derived from the same cross. We found that crossover frequencies on chromosome 3 are not statistically significantly different in individual intervals (Fisher's exact test with Bonferroni correction, $P > 0.008$, with 0.9 power to detect changes of 20–33% in crossover frequency, Table 1; Supplementary Tables 1 and 3 in File 1). There is a statistically significant increase of only 10% in overall map length for the chromosome (Table 1; Supplementary Tables 1 and 3 in File 1).

Because the regulation of recombination can be different between autosomes and sex chromosomes (Billmyre *et al.* 2019), we next asked if there is an interchromosomal effect on the X chromosome. We measured crossover frequencies on the X chromosome in *j3RM1* heterozygotes, *j2LM1* heterozygotes, and wildtype full siblings to *j2LM1*. We did not compare crossover frequencies to a wildtype full sibling of *j3RM1* because this stock is maintained over a *doublesex* mutation. Like chromosome 3, the crossover frequencies in individual intervals were not statistically different between inversion heterozygotes and the wildtype full sibling, nor was the entire map length (Fisher's exact test with Bonferroni correction, $P > 0.007$, with 0.9 power to detect changes of 27–45% in crossover frequency, Table 2; Supplementary Tables 2 and 3 in File 1).

D. melanogaster displays a range of interchromosomal effect sizes. A single inversion on one chromosome arm causes a 50% increase in a single centromere-spanning interval (Schultz and Redfield 1951) whereas multiply inverted balancer chromosomes cause a 50% increase in total map lengths (Joyce and McKim 2010). Our sample sizes are large enough to detect increases as small as 20% for an individual interval and 12% for entire map lengths (Supplementary Table 3 in File 1). While we cannot rule out that the interchromosomal effect in *D. simulans* might be below our detection limits, crossover frequencies actually decrease on the X chromosome in *j2LM1* heterozygotes, suggesting that there is no interchromosomal effect in *D. simulans*.

Heterozygous inversions do not cause a delay in oocyte specification

In *D. melanogaster*, meiosis occurs within the context of a 16-cell cyst that progresses through the germarium. Up to 4 nuclei within each cyst initiate meiosis by building synaptonemal complex (SC) in region 2a, but by region 2b only 2 nuclei remain in meiosis (the pro-oocytes), and by the end of the germarium in region 3, one of the pro-oocytes exits meiosis and the remaining cell is specified as the oocyte (Hughes *et al.* 2018). The RNA-binding protein Orb is essential for oocyte specification; this is reflected in the

Table 1. Crossover frequencies in cM for each interval along chromosome 3 in varying genotypes.

	Crossover frequencies (cM) on chromosome 3				
	jv–st	***st–e***	***e–p***	**Total**	***n***
Kenya	28.63 (25.75–31.52)	14.42 (12.18–16.66)	25.87 (23.08–28.67)	68.93 (68.04–69.82)	943
w^{501}	35.29 (32.01–38.56)	20.02 (17.28–22.77)	33.09 (29.87–36.31)	88.40 (87.51–89.29)	819
w; +/+	32.60 (29.81–35.38)	16.90 (14.47–19.12)	30.03 (27.31–32.75)	79.52 (78.63–80.42)	1089
w; +/*j2LM1*	36.00 (33.75–38.26)	18.83 (17.00–20.67)	32.91 (30.71–35.12)	87.75 (86.86–88.64)	1747
+/*j3RM1*	32.69 (28.99–36.38)	21.36 (18.13–24.59)	0	54.05 (53.15–54.94)	618

w; +/+ is the wildtype full sibling to *w*; +/*j2LM1*.
Values adjacent to cM are 95% confidence intervals. The variations in map length between Kenya, w^{501}, and the wildtype full sibling strain are statistically significantly different (χ^2, $P < 0.0001$).

Table 2. Crossover frequencies in cM for each interval along the X chromosome in varying genotypes.

	Crossover frequencies (cM) on chromosome X			
	y–v	***v–f***	**Total**	***n***
Kenya	42.95 (39.82–46.07)	23.86 (21.17–26.55)	66.8 (65.91–67.70)	964
w; +/+	39.90 (36.03–25.56)	29.15 (25.56–32.75)	69.06 (68.16–69.95)	614
w; +/*j2LM1*	42.38 (38.33–46.44)	25.04 (21.49–28.60)	67.43 (66.53–68.32)	571
+/*j3RM1*	45.35 (40.76–49.94)	30.31 (26.07–34.55)	75.66 (74.77–76.56)	452

w; +/+ is the wildtype full sibling to *w*; +/*j2LM1*.
Values adjacent to cM are 95% confidence intervals. No intervals are statistically significantly different (Fisher's exact test with Bonferroni correction for multiple tests). All *P*-values are shown in Supplementary Table 3 in File 1.

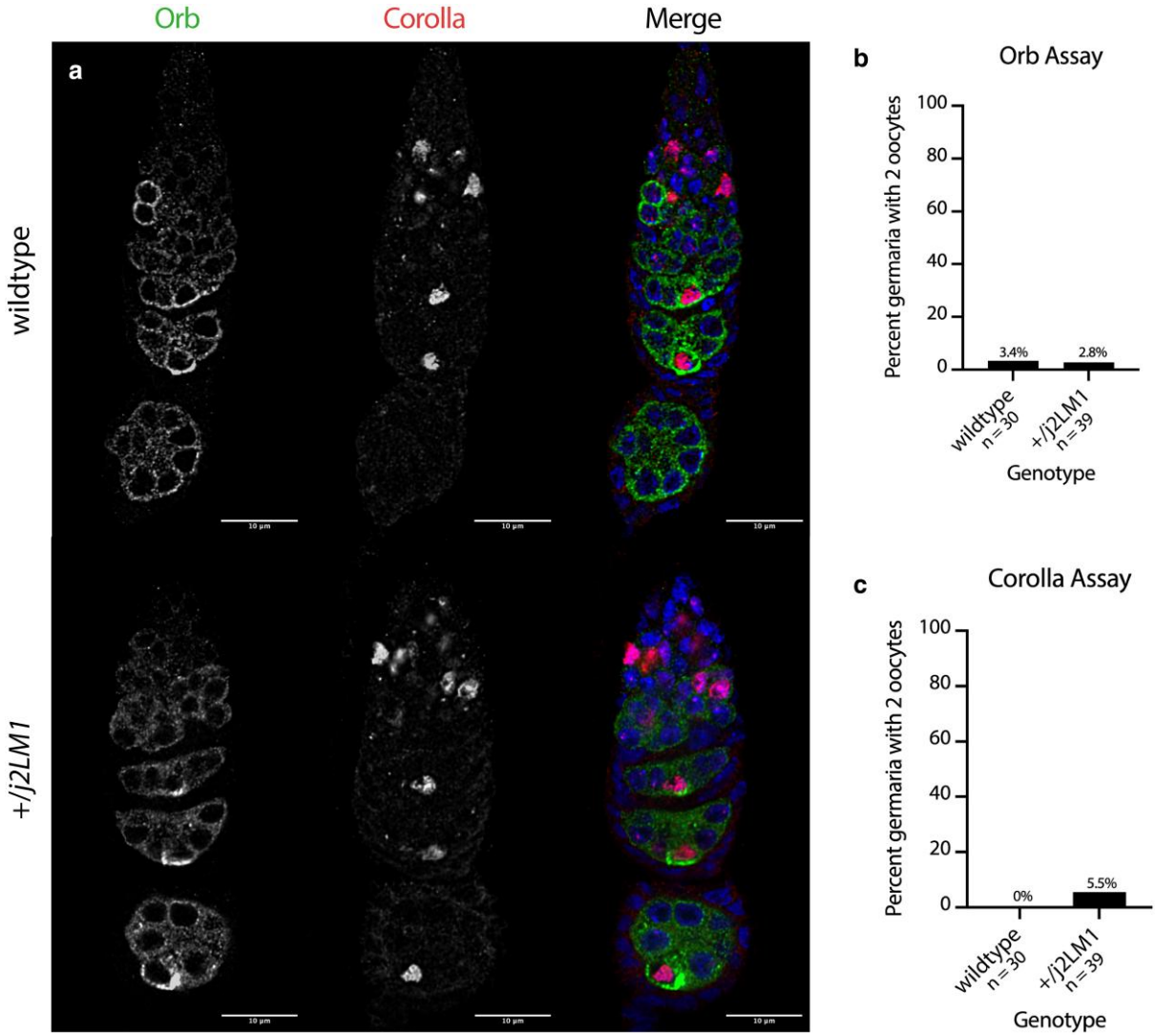

Fig. 3. Analysis of Orb and Corolla localization in full sibling wildtype and *j2LM1* heterozygotes shows no delay in oocyte specification. a) Immunofluorescence in *D. simulans* germaria and Stage 2 egg chambers with antibodies against Orb and Corolla in full sibling wildtype (top) and *+/j2LM1* heterozygotes (bottom). Orb accumulates in identical patterns to *D. melanogaster*. It first appears in the cytoplasm of all cells of a 16-cell cyst in region 2a. By region 2b, it has started to concentrate in the pro-oocytes, and by region 3 is concentrated in the designated oocyte. Different from *D. melanogaster*, Corolla is loaded onto full-length SC at the end of region 1, before Orb signal is detected. Note that because a single z-slice is shown, some signal is out of the focal plane and not all Corolla-positive nuclei are shown. b) and c) Quantification of the 2-oocyte phenotype using b) Orb localization and c) Corolla localization. There are no statistically significant differences in the frequency of the 2 oocytes in region 3 (Fisher's exact test, $P = 0.15$).

protein localization of Orb as it is initially present in the cytoplasm of all cells within a cyst beginning in region 2a but becomes concentrated in the oocyte during specification (Lantz *et al.* 1994). During the interchromosomal effect in *D. melanogaster*, heterozygous inversions activate the pachytene checkpoint, which monitors recombination intermediates and chromosome axes (Joyce and McKim 2009, 2010). Activating the pachytene checkpoint causes a prolonged prophase and a delay in oocyte specification, resulting in 2 Orb-positive oocytes instead of 1 in region 3 (Joyce and McKim 2010).

To ask if there is a 2-oocyte phenotype in inversion heterozygotes in *D. simulans*, we stained germarium with the *D. melanogaster* anti-Orb antibody (Lantz *et al.* 1994). While we do not have *orb* mutants in *D. simulans* to test for antibody specificity, the Orb staining pattern is identical to *D. melanogaster* (Fig. 3a). Like in *D. melanogaster*, Orb localizes to the cytoplasm of all cysts starting in region 2a, begins to concentrate in 2 cells starting in region 2b, and is concentrated in 1 cell only in region 3. In both the wildtype full sibling and *j2LM1* heterozygotes, only 3% of region 3 germaria had 2 oocytes (Fig. 3b). This again suggests that there is no interchromosomal effect in *D. simulans*.

During oocyte specification, one of the 2 pro-oocytes exits meiosis and disassembles the SC (Hughes *et al.* 2018). In *D. melanogaster*, the 2-oocyte phenotype can also be measured by the number of nuclei that have full length SC present in region 3. When measured this way, ~10% of the wildtype germaria have 2 SC-positive nuclei, but 50–90% of germaria in inversion heterozygotes have 2 SC -positive nuclei in region 3 (Joyce and McKim 2010). Since assaying for 2 oocytes using the SC as a marker is more sensitive than using Orb, we stained *D. simulans* germaria with the *D. melanogaster* antibody against the SC component Corolla (Fig. 3a). Although we do not have a *corolla* mutant to test for antibody specificity, we found that the nuclear staining pattern is identical to that in *D. melanogaster* and clearly identifies the SC in this

species (Fig. 3a). We also found that, like *D. melanogaster*, multiple cells within a cyst initiate meiosis and build SC, but by region 3, 100% of germaria had 1 nucleus with full-length SC. In the *j2LM1* heterozygotes, we saw the same pattern of Corolla staining as in wildtype. There was a marginal increase in the number of germaria with 2 Corolla-positive nuclei in region 3 (Fig. 3c), but this increase was not statistically significant (Fisher's exact test, $P = 0.15$).

It is possible that there is no pachytene checkpoint in *D. simulans*. If this were the case, then heterozygous inversions could not activate a pachytene checkpoint, leading to the absence of an interchromosomal effect. *pch2* is required for the pachytene checkpoint, so we aligned the predicted Pch2 protein sequences from *D. simulans* and *D. melanogaster* and found 94% sequence identity overall and 100% sequence identity in the predicted functional domains (Ye *et al.* 2015) (Supplementary Fig. 1 in File 1). While this level of amino acid identity suggests Pch2 is functional in *D. simulans*, it does not confirm the presence of a pachytene checkpoint.

Relationship between DSB formation and the SC in *D. simulans*

To understand the molecular reasons why there is no strong interchromosomal effect in *D. simulans*, we qualitatively analyzed the relationship between DNA DSB formation and the SC. In mouse and *S. cerevisiae*, SC formation is genetically dependent on DSB formation, while in *D. melanogaster* and *C. elegans*, SC formation is genetically independent of DSBs (Padmore *et al.* 1991; Dernburg *et al.* 1998; McKim *et al.* 1998; Baudat *et al.* 2000; Romanienko and Camerini-Otero 2000; Henderson and Keeney 2004). The relative relationship between the SC and DSB formation can result in very different physical environments where recombination occurs. In *D. melanogaster*, the timing of these events is such that the SC is fully assembled before DSBs form and thus recombination takes place within the context of a fully assembled SC (Mehrotra and McKim 2006). We reasoned that since the SC is thought to be important for implementing crossover patterning mechanisms, and that crossover patterning mechanisms are partially responsible for the interchromosomal effect (Crown *et al.* 2018), the relationship between DSBs and the SC might be different in *D. simulans* than in *D. melanogaster*.

We were able to qualitatively analyze the relative timing of DSB formation and synaptonemal formation in *D. simulans* through immunostaining. To visualize the SC, we stained with the *D. melanogaster* antibody against Corolla, a central region protein (Collins *et al.* 2014), and found staining consistent with that in *D. melanogaster* (Figs. 3 and 4). DSBs can be visualized cytologically using antibodies against phosphorylated H2AV (Mehrotra and McKim 2006; Lake *et al.* 2013). We tested the mouse monoclonal *D. melanogaster* antibody against phospho-H2AV (Lake *et al.* 2013) in *D. simulans* and, despite a moderate level of background staining, found a nuclear localization pattern consistent with that of meiotic DSBs in *D. melanogaster* (Fig. 4).

In *D. melanogaster*, the SC begins assembling in early region 2a at the same time as Orb appears, and full-length SC is present by late region 2a (Page and Hawley 2001; Takeo *et al.* 2011; Tanneti *et al.* 2011). Interestingly, in *D. simulans*, we found full-length Corolla staining at the end of region 1 before Orb appears (Fig. 3). It is possible that these nuclei are at the very end of zygotene and the cysts are on the cusp of entering Region 2a, but regardless of if they are late zygotene or early pachytene, the developmental timing of SC assembly in *D. simulans* represents a marked deviation from the timing in *D. melanogaster*. Additionally, the Corolla-positive nuclei always appear in pairs, suggesting that 2 cells per cyst enter meiosis (Fig. 4). Like *D. melanogaster*, full-length Corolla staining is visible in 2 nuclei in region 2b and in 1 nucleus in region 3 (Fig. 3).

In *D. melanogaster*, DSBs are initiated in region 2a quickly after the SC is fully assembled (Mehrotra and McKim 2006; Lake *et al.* 2013; Hughes *et al.* 2018). To determine the relative timing of DSB and SC formation in *D. simulans*, we analyzed phospho-H2AV patterns in the early germarium (Fig. 4). We observed that in pairs of nuclei in region 1 with full-length Corolla, 1 of the nuclei had strong phospho-H2AV signal while the other nucleus had weaker or no phospho-H2AV staining (Fig. 4, f and g). By region 2a, most Corolla-positive nuclei had robust phospho-H2AV staining (Fig. 4, a, b and d). We did detect nuclei with phospho-H2AV but without Corolla (Fig. 4, c and d, asterisks); these are most likely the future nurse cells as it is known that nurse cells undergo DSB formation in *D. melanogaster* (Mehrotra and McKim 2006). We repeated these same qualitative analyses in the *j2LM1* heterozgyotes and found no differences in the localization patterns of Corolla or phospho-H2AV (Fig. 4, i–p). We interpret these staining patterns such that full-length SC is built prior to robust DSB formation in *D. simulans*. Thus, while the relative timing of DSB and SC formation is similar between *D. melanogaster* and *D. simulans*, the early stages of prophase occur prior to Orb localization in *D. simulans*. Determining whether SC assembly is genetically dependent on DSB formation in *D. simulans* will require future genetic analyses.

Discussion

We set out to determine if there is an interchromosomal effect in *D. simulans* because the lack of inversions in wild and lab populations suggests it may be an interesting comparative model for understanding how heterozygous inversions shape gene flow dynamics and how, at the molecular level, mechanisms of recombination and crossover regulation might differ. We found no evidence supporting the presence of an interchromosomal effect in *D. simulans*, either genetically or cytologically. One limitation of our approach is that only one arm of chromosomes 2 or 3 were inverted. It is possible that crossovers were able to form on the chromosome arms that contained the standard arrangement and that a crossover on one arm of a chromosome prevents an interchromosomal effect. We do not think this is the case based on data from *D. melanogaster* showing a single inversion on chromosome 2L was able to cause a moderate interchromosomal effect (Schultz and Redfield 1951). Another limitation of our study is the large genetic intervals we used for determining crossover frequencies. There are a limited number of visible phenotypic markers available in *D. simulans* and, for the present study, we were limited to what is available. While the genetic intervals were large, they spanned regions of the chromosomes where the interchromosomal effect is the strongest in *D. melanogaster*—the pericentromeric and subtelomeric regions (Lucchesi and Suzuki 1968). In particular, the marker distribution on chromosome 3 would have been sufficient to detect increases in crossover frequencies across the centromere. The marker distribution on the X chromosome prevented us from detecting crossovers near the centromere, but the interchromosomal effect is strong at the distal end of the X chromosome in *D. melanogaster* and our markers did span that portion of the chromosome. Thus, the marker distribution was sufficient to detect an interchromosomal effect.

It is unclear what the function of the interchromosomal effect is. Is it an evolved response in species with high numbers of

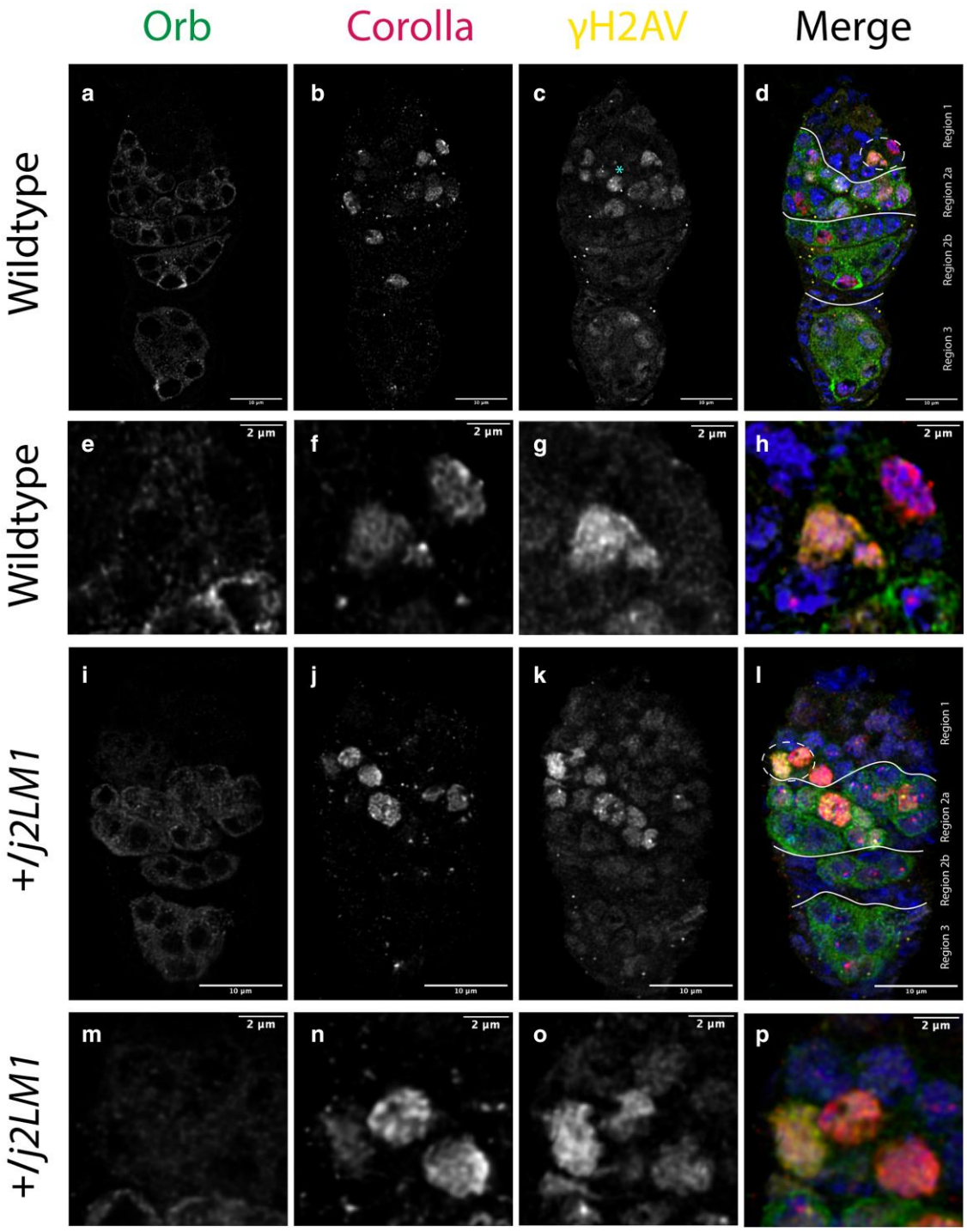

Fig. 4. Qualitative analysis of DSB and synaptonemal complex formation suggests the SC may form prior to DSB formation in *D. simulans*. a) to d) A single z-slice of a germarium from a wildtype full sibling showing full-length Corolla and phosphorylated H2AV in region 1 before Orb signal appears. Asterisks: Future nurse cell showing phosphorylated H2AV but no Corolla signal. Dashed circle: One of the nuclei in Region 1 has a phospho-H2AV signal, while the other nucleus shows none. e) to h) Higher magnification of nuclei in dashed circle in D. i) to l) Projection of 5 z-slices of a germarium from a *+/j2LM1* heterozygote showing full-length Corolla and phosphorylated H2AV in region 1 before Orb signal appears. Dashed circle: One of the nuclei in region 1 has a strong phospho-H2AV signal, while the other nucleus has a qualitatively weaker signal. m) to p) Higher magnification of nuclei in dashed circle in L.

segregating inversions or is it just an indirect result of checkpoint monitoring of normal meiotic processes? Looking at the interchromosomal effect in other Drosophila species can provide some insights. For example, *D. persimilis* and *D. pseudoobscura* are 2 hybridizing species with inversions between them; in interspecies crosses where the female hybrids are heterozygous for an inversion, there is a strong interchromosomal effect with characteristics similar to that in *D. melanogaster* (Stevison *et al.* 2011). Additionally, *D. robusta*, which has segregating inversions in natural populations, also displays an interchromosomal effect (Carson 1953; Lucchesi and Suzuki 1968). The work presented here is the first analysis of the interchromosomal effect in a monomorphic species and we have

shown that there is no interchromosomal effect, perhaps suggesting that the interchromosomal effect is not present in species where it is not needed. Future work analyzing the interchromosomal effect in other monomorphic species, such as *D. mauritiana* or *D. sechellia*, should give insights into this question (Krimbas and Powell 1992). Recent advances in high-efficiency CRISPR (Clustered Regularly Interspaced Short Palindromic Repeats) approaches make these experiments possible (Stern *et al.* 2023).

One possible mechanistic reason there is no interchromosomal effect in *D. simulans* is that crossover rates are higher in this species compared with *D. melanogaster* and there may simply not be much room for increasing crossover rates. True *et al* (1996) directly compared crossover rates in *D. melanogaster* and *D. simulans* using recessive marker scoring and found that the total genetic map length in *D. simulans* is 1.3 times longer than in *D. melanogaster*. More specifically, the total map length of the X chromosome is identical between species, but map lengths of chromosomes 2 and 3 are significantly longer. A more recent analysis used whole-genome sequencing to determine crossover rates in wild caught *D. melanogaster* and *D. simulans* trios (Wang *et al.* 2023). They found that overall crossover rates were 2.06 cM/Mb in a European population of *D. melanogaster*, 3.44 cM/Mb in a West African population of *D. melanogaster*, and 3.04 cM/Mb in a European *D. simulans* population.

Related to the increased rates of recombination is the observation that the centromere effect is weaker in *D. simulans*. In most species, crossovers are suppressed near centromeres—a phenomenon called the centromere effect (Pazhayam *et al.* 2021). Interestingly, True *et al.* (1996) showed that the centromere effect is weaker in *D. simulans* compared with *D. melanogaster*, and in fact, the increase in crossover frequencies in *D. simulans* can be mostly attributed to higher crossover frequencies across the centromere, as opposed to on the chromosome arms. Wang *et al.* (2023) were able to precisely map the location of crossovers using a sequencing approach and found that in *D. melanogaster*, the closest crossover to a centromere occurred 6.8 Mb away (of 177 crossovers examined), but in *D. simulans*, the closest crossover was 1.3 Mb from a centromere (of 109 crossovers examined). Together, these data suggest that the centromere effect is weaker in *D. simulans* than in *D. melanogaster*. The interchromosomal effect has the strongest impact on crossover frequencies in the centromere spanning intervals (Lucchesi and Suzuki 1968), thus it could be possible that if there is a weaker centromere effect in *D. simulans* —that is, crossovers are already higher in these regions—there simply is no room to increase crossover rates.

Assessing the interchromosomal effect cytologically allows us to rule out higher crossover rates as the reason there is no interchromosomal effect. The interchromosomal effect in *D. melanogaster* is caused by activating the pachytene checkpoint, which then allows more crossovers to form (Joyce and McKim 2010). If heterozygous inversions activate the pachytene checkpoint in *D. simulans*, but more crossovers do not form because crossover rates are already at or near a maximum level, we still would have detected the 2-ooctye phenotype. Thus, we do not think higher crossover rates and a weaker centromere effect are the reason there is no interchromosomal effect in *D. simulans*.

Another mechanistic reason there might not be an interchromosomal effect in *D. simulans* is that the pachytene checkpoint might not be present. *pch2* is the gene required for the pachytene checkpoint in *D. melanogaster*, so we aligned the predicted Pch2 protein sequences from *D. simulans* and *D. melanogaster* and found 94% sequence identity and 100% sequence identity in the predicted domains of Pch2 (Ye *et al.* 2015) (Supplementary Fig. 1 File 1). While there could be mutations in other genes required for the checkpoint, there at least appears to be a functional orthologue of *pch2* in *D. simulans*.

We asked if there are differences in the timing of DSB and SC formation that might explain why there is no interchromosomal effect in *D. simulans*. At the resolution of immunostaining, we found that the SC forms before DSBs as it does in *D. melanogaster*. However, there is a clear difference in the developmental timing of zygotene in *D. simulans* because the SC is fully assembled before Orb localization. The pachytene checkpoint delays oocyte specification and extends the window during which crossovers can form, ultimately leading to higher crossover rates during the interchromosomal effect (Joyce and McKim 2010). The correlation between oocyte specification and meiotic chromosome dynamics raises the possibility that crossover control mechanisms are active during certain developmental windows that are related to, or can be marked by, oocyte specification. If the initial steps of crossover and SC formation occur prior to that developmental window in *D. simulans*, then perhaps this prevents checkpoint activation and an interchromosomal effect. This hypothesis remains to be tested and will require an in-depth characterization of meiosis in *D. simulans*.

Data availability

All stocks are available upon request. The authors affirm that all data necessary for confirming the conclusions of the article are present within the article, figures, and tables. Sequencing data are deposited at NCBI BioProject ID PRJNA1110566.

Supplemental material is available at GENETICS online.

Acknowledgments

We thank Scott Hawley for antibodies, Amanda Larracuente for stocks, and the National Drosophila Species Stock Center for stocks.

Funding

This work was supported by NIH grant R35GM137834 to KNC. DLS is an employee of the Howard Hughes Medical Institute. The funders had no role in the design of the study or in data collection, analysis, and interpretation or in writing of the study.

Conflicts of interest

The author(s) declare no conflict of interest.

Literature cited

Altschul SF, Gish W, Miller W, Myers EW, Lipman DJ. 1990. Basic local alignment search tool. J Mol Biol. 215(3):403–410. doi:10.1016/S0022-2836(05)80360-2.

Andolfatto P, Davison D, Erezyilmaz D, Hu TT, Mast J, *et al.* 2011. Multiplexed shotgun genotyping for rapid and efficient genetic mapping. Genome Res. 21(4):610–617. doi:10.1101/gr.115402.110.

Aulard S, Monti L, Chaminade N, Lemeunier F. 2004. Mitotic and polytene chromosomes: comparisons between *Drosophila melanogaster* and *Drosophila simulans*. Genetica. 120(1–3):137–150. doi:10.1023/B:GENE.0000017637.10230.c4.

Baudat F, Manova K, Yuen JP, Jasin M, Keeney S. 2000. Chromosome synapsis defects and sexually dimorphic meiotic progression in

mice lacking Spo11. Mol Cell. 6(5):989–998. doi:10.1016/S1097-2765(00)00098-8.
Billmyre KK, Cahoon CK, Heenan GM, Wesley ER, Yu Z, *et al.* 2019. X chromosome and autosomal recombination are differentially sensitive to disruptions in SC maintenance. Proc Natl Acad Sci. 116(43):21641–21650. doi:10.1073/pnas.1910840116.
Carson HL. 1953. The effects of inversions on crossing over in *Drosophila robusta*. Genetics. 38(2):168–186. doi:10.1093/genetics/38.2.168.
Collins KA, Unruh JR, Slaughter BD, Yu Z, Lake CM, *et al.* 2014. Corolla is a novel protein that contributes to the architecture of the synaptonemal complex of *Drosophila*. Genetics. 198(1):219–228. doi:10.1534/genetics.114.165290.
Courret C, Chang C-H, Wei KHC, Montchamp-Moreau C, Larracuente AM. 2019. Meiotic drive mechanisms: lessons from *Drosophila*. Proc R Soc B: Biol Sci. 286(1913):20191430. doi:10.1098/rspb.2019.1430.
Courret C, Larracuente AM. 2023. High levels of intra-strain structural variation in *Drosophila simulans* X pericentric heterochromatin. Genetics. 225(4):iyad176. doi:10.1093/genetics/iyad176.
Crown KN, Miller DE, Sekelsky J, Hawley RS. 2018. Local inversion heterozygosity alters recombination throughout the genome. Curr Biol. 28(18):2984–2990.e3. doi:10.1016/j.cub.2018.07.004.
Dernburg AF, McDonald K, Moulder G, Barstead R, Dresser M, *et al.* 1998. Meiotic recombination in *C. elegans* initiates by a conserved mechanism and is dispensable for homologous chromosome synapsis. Cell. 94(3):387–398. doi:10.1016/S0092-8674(00)81481-6.
Faul F, Erdfelder E, Lang A-G, Buchner A. 2007. G*Power 3: a flexible statistical power analysis program for the social, behavioral, and biomedical sciences. Behav Res Methods. 39(2):175–191. doi:10.3758/BF03193146.
Grell RF. 1964. Chromsoome size at distributive pairing in *Drosophila melanogaster* females. Genetics 50(1): 151–166. doi:10.1093/genetics/50.1.151.
Henderson KA, Keeney S. 2004. Tying synaptonemal complex initiation to the formation and programmed repair of DNA double-strand breaks. Proc Natl Acad Sci. 101(13):4519–4524. doi:10.1073/pnas.0400843101.
Hughes SE, Miller DE, Miller AL, Hawley RS. 2018. Female meiosis: synapsis, recombination, and segregation in *Drosophila melanogaster*. Genetics. 208(3):875–908. doi:10.1534/genetics.117.300081.
Hunter CM, Huang W, Mackay TFC, Singh ND. 2016. The genetic architecture of natural variation in recombination rate in *Drosophila melanogaster*. PLoS Genet. 12(4):e1005951. doi:10.1371/journal.pgen.1005951.
Inoue Y. 1988. Chromosomal mutation in *Drosophila melanogaster* and *Drosophila simulans*. Mutat Res/Fundam Mol Mech Mutagen. 197(1):85–92. doi:10.1016/0027-5107(88)90143-1.
Joyce EF, McKim KS. 2009. Drosophila PCH2 is required for a pachytene checkpoint that monitors double-strand-break-independent events leading to meiotic crossover formation. Genetics. 181(1):39–51. doi:10.1534/genetics.108.093112.
Joyce EF, McKim KS. 2010. Chromosome axis defects induce a checkpoint-mediated delay and interchromosomal effect on crossing over during Drosophila meiosis. PLoS Genet. 6(8):e1001059. doi:10.1371/journal.pgen.1001059.
Krimbas C, Powell JR. 1992. Drosophila Inversion Polymorphism. Boca Raton (FL): CRC Press.
Lake CM, Korda Holsclaw J, Bellendir SP, Sekelsky J, Hawley RS. 2013. The development of a monoclonal antibody recognizing the *Drosophila melanogaster* phosphorylated histone H2A variant (γ-H2AV). G3 (Bethesda). 3:1539–1543. doi:10.1534/g3.113.006833.
Lantz V, Chang JS, Horabin JI, Bopp D, Schedl P. 1994. The *Drosophila* orb RNA-binding protein is required for the formation of the egg chamber and establishment of polarity. Genes Dev. 8:598–613. doi:10.1101/gad.8.5.598.
Lemke D, Tonzetich J, Shumeyko M. 1978. Resistance to radiation induced chromosomal rearrangements in *Drosophila simulans*. Drosoph Inf Ser. 53:159–161.
Lucchesi JC, Suzuki DT. 1968. The interchromosomal control of recombination. Annu Rev Genet. 2:53–86. doi:10.1146/annurev.ge.02.120168.000413.
McKim KS, Green-Marroquin BL, Sekelsky JJ, Chin G, Steinberg C, *et al.* 1998. Meiotic synapsis in the absence of recombination. Science. 279:876–878. doi:10.1126/science.279.5352.876.
Mehrotra S, McKim KS. 2006. Temporal analysis of meiotic DNA double-strand break formation and repair in *Drosophila* females. PLoS Genet. 2:e200. doi:10.1371/journal.pgen.0020200.
Miller DE. 2020. The interchromosomal effect: different meanings for different organisms. Genetics. 216:621–631. doi:10.1534/genetics.120.303656.
Noor MA, Grams KL, Bertucci LA, Reiland J. 2001. Chromosomal inversions and the reproductive isolation of species. Proc Natl Acad Sci. 98:12084–12088. doi:10.1073/pnas.221274498.
Padmore R, Cao L, Kleckner N. 1991. Temporal comparison of recombination and synaptonemal complex formation during meiosis in *S. cerevisiae*. Cell. 66:1239–1256. doi:10.1016/0092-8674(91)90046-2.
Page SL, Hawley RS. 2001. C(3)G encodes a *Drosophila* synaptonemal complex protein. Genes Dev. 15:3130–3143. doi:10.1101/gad.935001.
Pazhayam NM, Turcotte CA, Sekelsky J. 2021. Meiotic crossover patterning. Front Cell Dev Biol. 9:681123. doi:10.3389/fcell.2021.681123.
Picelli S, Björklund ÅK, Reinius B, Sagasser S, Winberg G, *et al.* 2014. Tn5 transposase and tagmentation procedures for massively scaled sequencing projects. Genome Res. 24:2033–2040. doi:10.1101/gr.177881.114.
Powell JR. 1997. Progress and Prospects in Evolutionary Biology: the Drosophila Model. New York (NY): Oxford University Press.
Rieseberg LH. 2001. Chromosomal rearrangements and speciation. Trends Ecol Evol. 16:351–358. doi:10.1016/S0169-5347(01)02187-5.
Romanienko PJ, Camerini-Otero RD. 2000. The mouse *Spo11* gene is required for meiotic chromosome synapsis. Mol Cell. 6:975–987. doi:10.1016/S1097-2765(00)00097-6.
Schultz J, Redfield H. 1951. Interchromosomal effects on crossing over in *Drosophila* Cold Spring Harbor symposia on quantitative. Biology (Basel). 16:175–197. doi:10.1101/SQB.1951.016.01.015.
Stern DL. 2022. Transgenic tools for targeted chromosome rearrangements allow construction of balancer chromosomes in non-melanogaster *Drosophila* species. G3 (Bethesda). 12:jkac030. doi:10.1093/g3journal/jkac030.
Stern DL, Crocker J, Ding Y, Frankel N, Kappes G, *et al.* 2017. Genetic and transgenic reagents for *Drosophila simulans*, *D. Mauritiana*, D. Yakuba, *D. Santomea*, and *D. Virilis*. G3 (Bethesda). 7:1339–1347. doi:10.1534/g3.116.038885.
Stern DL, Kim E, Berhman EL. 2023 The Janelia Atalanta plasmids provide a simple and efficient CRISPR/Cas9-mediated homology directed repair platform for Drosophila. bioRxiv 545412. https://doi.org/10.1101/2023.06.17.545412, preprint: not peer reviewed.
Stevison LS, Hoehn KB, Noor MAF. 2011. Effects of inversions on within- and between-species recombination and divergence. Genome Biol Evol. 3:830–841. doi:10.1093/gbe/evr081.
Stone W, Thomas I. 1935. Crossover and disjunctional properties of X chromosome inversions in *Drosophila melanogaster*. Genetica. 17:170–184. doi:10.1007/BF01984187.
Sturtevant AH. 1926. A crossover reducer in *Drosophila melanogaster* due to inversion of a section of the third chromosome. Biol Zentralbl. 46:697–702.

Sturtevant AH, Beadle GW. 1936. The relations of inversions in the X chromosome of *Drosophila melanogaster* to crossing over and disjunction. Genetics. 21:554–604. doi:10.1093/genetics/21.5.554.

Takeo S, Lake CM, Morais-de-Sá E, Sunkel CE, Hawley RS. 2011. Synaptonemal complex-dependent centromeric clustering and the initiation of synapsis in *Drosophila* oocytes. Curr Biol. 21: 1845–1851. doi:10.1016/j.cub.2011.09.044.

Tanneti NS, Landy K, Joyce EF, McKim KS. 2011. A pathway for synapsis initiation during zygotene in *Drosophila* oocytes. Curr Biol. 21:1852–1857. doi:10.1016/j.cub.2011.10.005.

True JR, Mercer JM, Laurie CC. 1996. Differences in crossover frequency and distribution among three sibling species of *Drosophila*. Genetics. 142:507–523. doi:10.1093/genetics/142.2.507.

Wang Y, McNeil P, Abdulazeez R, Pascual M, Johnston SE, *et al.* 2023. Variation in mutation, recombination, and transposition rates in *Drosophila melanogaster* and *Drosophila simulans*. Genome Res. 33: 587–598. doi:10.1101/gr.277383.122.

Woodruff RC, Ashburner M. 1978. The frequency of x-ray-induced chromosome breakage in the sibling species *Drosophila melanogaster* and *Drosophila simulans*. Am Nat. 112:456–459. doi:10.1086/283289.

Ye Q, Rosenberg SC, Moeller A, Speir JA, Su TY, *et al.* 2015. TRIP13 is a protein-remodeling AAA+ ATPase that catalyzes MAD2 conformation switching. Elife. 4:e07367. doi:10.7554/eLife.07367.

Editor: A. Larracuente